Reorganization Energy of the Initial Electron-Transfer Step in Photosynthetic Bacterial Reaction Centers

William W. Parson,* Zhen Tao Chu,# and Arieh Warshel#
*Department of Biochemistry, University of Washington, Seattle, Washington 98195-7350, and #Department of Chemistry, University of Southern California, Los Angeles, California 90007 USA

ABSTRACT The reorganization energy (λ) for electron transfer from the primary electron donor (P*) to the adjacent bacteriochlorophyll (B) in photosynthetic bacterial reaction centers is explored by molecular-dynamics simulations. Relatively long (40 ps) molecular-dynamics trajectories are used, rather than free energy perturbation techniques. When the surroundings of the reaction center are modeled as a membrane, λ for $P^*B \rightarrow P^+B^-$ is found to be ~1.6 kcal/mol. The results are not sensitive to the treatment of the protein's ionizable groups, but surrounding the reaction center with water gives higher values of λ (~6.5 kcal/mol). In light of the evidence that P^+B^- lies slightly below P* in energy, the small λ obtained with the membrane model is consistent with the speed and temperature independence of photochemical charge separation. The calculated reorganization energy is smaller than would be expected if the molecular dynamics trajectories had sampled the full conformational space of the system. Because the system does not relax completely on the time scale of electron transfer, the λ obtained here probably is more pertinent than the larger value that would be obtained for a fully equilibrated system.

INTRODUCTION

The initial charge-separation reaction in photosynthetic bacterial reaction centers is the transfer of an electron from an electronically excited bacteriochlorophyll dimer (P*) to a bacteriopheophytin (H). The reaction generates a P^+H^- ion pair with a time constant of ~3 ps at room temperature, and it becomes even faster at cryogenic temperatures (Woodbury et al., 1985; Breton et al., 1988; Fleming et al., 1988). Recent experimental work has provided increasing support for the view that charge separation occurs in two distinct steps (Holzapfel et al., 1990; Arlt et al., 1993, 1996; Shkuropatov and Shuvalov, 1996; Maiti et al., 1994; Schmidt et al., 1994, 1995; Heller et al., 1995, 1996; Kirmaier et al., 1995a,b; Holzwarth and Muller, 1996; Van Brederode et al., 1996; Kennis et al., 1997). In the first step, P* probably transfers an electron to a neighboring bacteriochlorophyll (B), forming a P^+B^- ion pair; in the second step, an electron moves from B^- to H:

$$PBH \xrightarrow{h\nu} P^*BH \rightleftarrows P^+B^-H \rightleftarrows P^+BH^-$$

The relative energies of P*, P^+B^-, and P^+H^- have been explored by both experimental and theoretical approaches. The overall free energy change ($\Delta G°$) for the formation of P^+H^- from P* is measured to be in the range of -5 to -6 kcal/mol at 295 K (Woodbury and Parson, 1984; Goldstein et al., 1998; Ogrodnik et al., 1988, 1994). However, P^+H^- appears to be created much closer in energy to P* and to relax toward its final level on both the picosecond and nanosecond time scales (Woodbury and Parson, 1984; Ogrodnik et al., 1988; Peloquin et al., 1994; Woodbury et al., 1994; Holzwarth and Muller, 1996). Measurements of the kinetics of charge separation in mutant or chemically modified reaction centers suggest that $\Delta G°$ for the formation of P^+B^- in wild-type reaction centers is on the order of -0.4 to -2 kcal/mol (Nagarajan et al., 1993; Jia et al., 1993; Hamm et al., 1993; Shkuropatov and Shuvalov, 1996; Schmidt et al., 1994; Huber et al., 1995; Arlt et al., 1996; Heller et al., 1996; Bixon et al., 1996; Van Brederode et al., 1996; Kennis et al., 1997). Electrostatics and molecular dynamics/free energy perturbation (FEP) calculations based on the crystallographic structure of the reaction center have put P^+B^- ~3 kcal/mol below P*, with an estimated uncertainty of ±3 kcal/mol (Parson et al., 1990; Warshel et al., 1994; Alden et al., 1995, 1996a,b). Calculations that place $P^+B_L^-$ above P* in energy have been described (Marchi et al., 1993; Gunner et al., 1996), but some of these estimates appear to be based on an oversimplified treatment of dielectric effects (see Alden et al., 1995, 1996a).

The reactions $P^*B \rightarrow P^+B^-$ and $P^+B^-H \rightarrow P^+BH^-$ thus occur on the time scale of 1–10 ps, involve only small changes in free energy, and have very small or negative activation energies. This combination of properties requires that the reorganization energy (λ) for each reaction be comparable in magnitude to $\Delta G°$, which means that it must be on the order of 1–3 kcal/mol. The reorganization energy is the energy required to distort the system from the most probable configuration of the reactant state to the most probable configuration of the reactants. In the classical Marcus theory (Marcus, 1956, 1996), the activation energy of an electron-transfer reaction is given by $\Delta g^{\ddagger} = (\Delta G° + \lambda)^2/4\lambda$, which goes to zero when $\lambda = -\Delta G°$. Bixon et al. (1996), who used a quantum mechanical expression to fit the kinetics of charge separation in a selected series of

Received for publication 6 August 1997 and in final form 21 October 1997.
Address reprint requests to Dr. W. Parson, Department of Biochemistry, Box 357350, University of Washington, Seattle, WA 98195-7350. Tel.: 206-543-1743; Fax: 206-685-1792; E-mail: parsonb@u.washington.edu.

0006-3495/98/01/182/10 $2.00

mutant and modified reaction centers, estimated $\Delta G°$ for $P^*B \rightarrow P^+B^-$ to be -1.4 ± 0.5 kcal/mol, and found the "medium" reorganization energy to be 2.3 ± 0.7 kcal/mol. Other investigators have suggested overall values of λ ranging from 2.0 (Nagarajan et al., 1993) to less than 0.7 kcal/mol (Williams et al., 1992; Hamm et al., 1993; Jia et al., 1993; Murchison et al., 1993). Some of the variation among these estimates could be related to the general issue of defining the effective reorganization energy for a process that occurs on a very short time scale; we will return to this point below.

For electron transfer between large molecules such as bacteriochlorophyll, in which small changes in atomic charges are distributed over many atoms of the π systems, internal vibrational modes of the electron carriers are expected to make relatively minor contributions to λ. The more important medium reorganization energy (λ_o) reflects reorganization of the surrounding protein and solvent. In a simple, macroscopic model, λ_o for a one-electron transfer reaction depends on the center-to-center distance between the electron carriers (R), the radii of the electron donor and acceptor (a_1 and a_2), and the optical (ϵ_{op}) and low-frequency (ϵ) dielectric constants of the medium (Marcus, 1956, 1996):

$$\lambda_o = (332 \text{ kcal/mol})\left(\frac{1}{2a_1} + \frac{1}{2a_2} - \frac{1}{R}\right)\left(\frac{1}{\epsilon_{op}} - \frac{1}{\epsilon}\right) \quad (1)$$

This expression shows qualitatively that λ_o can be small if the electron carriers are close together ($R \approx a_1 + a_2$) and if the effective ϵ approaches ϵ_{op}, which means that the surrounding molecules are nonpolar or cannot move significantly in response to the electric field from the ion pair. However, Eq. 1 is of limited use for reactions in a protein, where the local structure and dielectric "constant" around the electron carriers can be highly anisotropic and there is no unique prescription for determining ϵ or the radii a_1 and a_2 (see discussion in King et al., 1991, and Muegge et al., 1997).

Previous attempts to calculate the reorganization energies for the photosynthetic charge separation steps on the basis of the reaction center's crystal structure have not been entirely successful. Early calculations gave values of 3–4 kcal/mol (Creighton et al., 1988; Parson et al., 1990). More recent FEP calculations that generated what appear to be approximately the correct energies for P^+B^- and P^+H^- yielded reorganization energies of 5 kcal/mol or more, depending on whether internal cavities of the protein were assumed to be occupied by water (Warshel et al., 1994; Alden et al., 1995). However, it was pointed out that the FEP treatment could have forced the system to undergo more extensive relaxations than would actually occur on the time scale of the electron transfer reactions (Alden et al., 1995).

The rate constant for an electron transfer process is determined by the probability per unit time that a trajectory in the reactant state will reach a point where the potential energy surfaces of the reactant and product states intersect (Warshel and Parson, 1991; Parson and Warshel, 1995). In the FEP approach, this probability is calculated by using umbrella sampling to sample the entire configuration space of the system (Hwang and Warshel, 1987; Kuharski et al., 1988; King and Warshel, 1990; Warshel and Parson, 1991; Kollman, 1993). Such sampling provides a free energy function of the reaction coordinate, from which the reorganization energy can be obtained straightforwardly. However, it is not clear that the FEP approach will return the correct probability of reaching the transition state in the case of an extremely fast reaction, when the reaction time can be shorter than the conformational relaxation time of the system. Configurations that are not accessed on the time scale of the reaction would not be expected to affect the kinetics. We address this issue in the present work by using relatively long molecular dynamics trajectories rather than FEP. Several models of the reaction center and the surrounding medium are considered to assess the sensitivity of the calculated λ to the model.

METHODS

Theoretical approach

The time evolution of an electron transfer process in a condensed phase can be simulated by several approaches. The diabatic limit can be explored semiclassically by surface-hopping approaches (Warshel, 1982; Warshel and Hwang, 1985, 1986; Warshel and Parson, 1991), or quantum mechanically by the dispersed-polaron/spin-boson model (Warshel and Hwang, 1986; Warshel et al., 1989; Schulten and Tesch, 1991; Marchi et al., 1993). For a recent discussion of the identity of the dispersed-polaron and spin-boson models, see Hwang and Warshel (1997). Path integral methods (Egger and Mak, 1993, 1994; Makri et al., 1996) can be used to study the quantum mechanical time evolution of rapid electron transfer in both the diabatic and adiabatic limits, as can density matrix methods, once the spectral distribution of vibrations coupled to the reaction has been obtained by dispersed-polaron simulations (Warshel and Parson, 1991; Parson and Warshel, 1995). Here we use the semiclassical approach as a starting point.

The semiclassical rate constant for electron transfer can be evaluated by extending the surface-hopping model (Tully and Preston, 1971; Miller and George, 1972) to condensed phases (Warshel, 1982; Warshel and Hwang, 1985, 1986; Creighton et al., 1988; Warshel and Parson, 1991; Webster et al., 1994). This approach involves running molecular dynamics trajectories on the potential surface of the reactant state (V_1) and monitoring the potential energy difference between the reactant and product states ($\Delta V(t) = V_2(t) - V_1(t)$). If the wavefunction of the system is written as a

linear combination of wavefunctions for the two states, with coefficients C_1 and C_2, the rate constant for a nonadiabatic transition from state 1 to state 2 is given by

$$k_{12} \approx \lim_{t\to\infty}\{\langle|C_2(t)|^2\rangle_1 t^{-1}\} \tag{2}$$

$$C_2(t) = \int_0^t (-iH_{12}/\hbar)C_1(\tau)\exp\left\{(-i/\hbar)\int_0^\tau \Delta V(\tau')d\tau'\right\}d\tau \tag{3}$$

Here $\langle\cdots\rangle_s$ means an average over many trajectories (or one sufficiently long trajectory) in state s; H_{12} is the electronic interaction matrix element between the two states; and the coefficient for state 1 (C_1) is assumed to remain near 1.0. Equation 3 neglects interference effects on the assumption that systems that cross to the product state dephase electronically before they return to the reactant state. This assumption is justified by simulations showing that $|\Delta V(t)|$ increases very rapidly once a trajectory crosses to the product state and begins to relax on the potential of that state (Warshel and Hwang, 1985, 1986). When $|\Delta V(t)|$ is large, the integrand in Eq. 3 oscillates rapidly and makes little contribution to k_{12}.

Analysis of Eqs. 2 and 3 shows that k_{12} is determined by the probability per unit time that a trajectory in state 1 will reach a point where $\Delta V(t) = 0$ (Warshel, 1982; Tachiya, 1989). The activation free energy ($\Delta g^\ddagger$) reflects the intersection of two free energy surfaces, Δg_1 and Δg_2, which express (in units of free energy) the probabilities of finding various values of ΔV during trajectories on V_1 and V_2, respectively. The free energy function for state 1 can be obtained by running a molecular dynamics trajectory on V_1 and sorting the number of times that each value of ΔV is found. If the trajectory is long enough to span the complete configurational space of the system, the normalized probability $\bar{\mathcal{P}}_1(\Delta V')$ that $\Delta V(t)$ will be equal to the particular value $\Delta V'$ at any given time during the trajectory is (King and Warshel, 1990; Zhou and Szabo, 1995)

$$\begin{aligned}\bar{\mathcal{P}}_1(\Delta V') &= \exp\{-\Delta g_1(\Delta V')\beta\} = N\langle\delta(\Delta V - \Delta V')\rangle_1 \\ &= \frac{N\int \delta(\Delta V - \Delta V')\exp\{-V_1\beta\}d\Gamma}{\int \exp\{-V_1\beta\}d\Gamma}\end{aligned} \tag{4}$$

where $\beta = 1/RT$, $\delta(\Delta V - \Delta V')$ is the Dirac delta function, $N = 1/\langle\delta(\Delta V - \Delta V_o)\rangle_1$, $\Delta V_o = \langle\Delta V\rangle_1$, and Γ is a generalized configurational coordinate. The free energy gap $\Delta V'$ thus can be used as a generalized reaction coordinate for the probabilities and free energy functions. The free energy function for state 1 is $\Delta g_1(\Delta V') = -RT\ln\{\bar{\mathcal{P}}_1(\Delta V')\}$.

To obtain $\Delta g^\ddagger$ and λ, we also need Δg_2. Although Δg_2 can be calculated from a similar trajectory on the potential surface of state 2 (vide infra), an alternative route becomes apparent if Eq. 4 is rewritten as

$$\begin{aligned}&\exp\{-\Delta g_1(\Delta V')\beta\} \\ &= \frac{N\int \delta(\Delta V - \Delta V')\exp\{-(V_1 - V_2)\beta\}\exp\{-V_2\beta\}d\Gamma}{\int \exp\{-V_1\beta\}d\Gamma} \\ &= \frac{N\int \delta(\Delta V - \Delta V')\exp\{-\Delta V'\beta\}\exp\{-V_2\beta\}d\Gamma}{\int \exp\{-V_1\beta\}d\Gamma} \\ &= \exp\{-\Delta V'\beta\}\left(\frac{\int \exp\{-V_2\beta\}d\Gamma}{\int \exp\{-V_1\beta\}d\Gamma}\right) \\ &\qquad \frac{N\int \delta(\Delta V - \Delta V')\exp\{-V_2\beta\}d\Gamma}{\int \exp\{-V_2\beta\}d\Gamma} \\ &= \exp\{-\Delta V'\beta\}\exp\{-\Delta g_2(\Delta V')\beta\}\end{aligned} \tag{5}$$

with $\Delta g_2(\Delta V') = \Delta G^\circ - \beta^{-1}\ln\{\bar{\mathcal{P}}_2(\Delta V')\}$ and $\Delta G^\circ = -\beta^{-1}\ln\{\int \exp\{-V_2\beta\}d\Gamma/\int \exp\{-V_1\beta\}d\Gamma\}$. Equation 5 leads to the relationship

$$\Delta g_2(\Delta V') = \Delta g_1(\Delta V') + \Delta V' \tag{6}$$

which allows $\Delta g_2(\Delta V')$ to be calculated immediately from $\Delta g_1(\Delta V')$. This relationship has been pointed out previously (Warshel, 1982; Tachiya, 1989) and has been obtained by an alternative derivation by King and Warshel (1990).

Equation 6 states that, for any given value of the reaction coordinate $\Delta V'$, the free energy difference between the two electronic states is $\Delta V'$. It may seem surprising that a free energy difference can be expressed in this way, when the time-dependent $\Delta V(t)$ is simply an energy. It is important to note in this connection that the reaction coordinate $\Delta V'$ in Eqs. 4–6 is not $\Delta V(t)$, but rather the parameter used for sorting the probabilities that $\Delta V(t)$ falls within various brackets ($\Delta V' \pm \delta$) during a molecular dynamics trajectory. Sorting over a sufficiently long trajectory provides a Boltzmann average over all of the conformational states of the system. Note, however, that Eqs. 5 and 6 are rigorously correct only if the molecular dynamics trajectory on V_1 properly samples the entire conformational space, which in principle requires that the trajectory be infinitely long. Short trajectories are likely to provide biased sampling.

The problem of incomplete sampling can be reduced significantly by the FEP approach, which drives the system to the relevant conformations, even if they require high values of V_1. This approach appears to be the only alternative in studies of reactions with large activation energies, where there is otherwise no chance of reaching the transition state in finite simulation time. For reactions that occur within a few picoseconds, however, the probability of visiting the transition state can be appreciable. In these cases, Δg_1 and Δg_2 can be obtained directly from separate simulations on V_1 and V_2. Values of $\Delta g^\ddagger$ and λ derived from

these free energy functions should be more pertinent than values obtained with the FEP procedure, because the simulations are more likely to sample only the configurations that are accessible on the time scale of the actual reaction. Differences between values of λ obtained by the two approaches can be considered to reflect dynamic effects. When the two approaches give different reorganization energies, we would not expect the Δg_1 and Δg_2 obtained by separate trajectories on V_1 and V_2 to satisfy Eq. 6.

Implementation

To evaluate the probability distributions defined by Eq. 4, we carried out molecular dynamics simulations with a modified version of the program Enzymix (Lee and Warshel, 1992; Lee et al., 1993; Warshel et al., 1994; Alden et al., 1995, 1996b). The *Rhodopseudomonas viridis* crystal structure (Deisenhofer et al., 1995) was trimmed to 23 Å around a point midway between the electron donor (P) and acceptor (B). To represent the surrounding membrane, solvent, and more distant parts of the protein, the trimmed protein was embedded in a sphere containing induced dipoles on a grid with a 4-Å grid spacing. The sphere had a radius of 29 Å. The distances between the Mg atoms of the BChls and the N_ϵ atoms of the His axial ligands were constrained by a harmonic potential (50 kcal/Å^2) at their crystallographic values. The O atoms of the crystallographic water molecules also were given a weak harmonic constraint (5 kcal/Å^2) around their crystallographic coordinates. (This was necessary because the model did not include explicit bulk water molecules to replace water molecules that diffused out of the protein during the simulations. The constraint kept the crystallographic waters in the vicinity of their original positions, while allowing excursions of several Å around these points.) Otherwise, unconstrained atomic motions were allowed in the region within 21 Å from the center of the system, and motions with harmonic constraints (Warshel et al., 1986) were allowed at the crystallographic positions outside this region. The local reaction field method (Lee and Warshel, 1992; Lee et al., 1993) was used to treat all atoms in the 23-Å structure explicitly, with no cutoff distance for long-range electrostatic interactions. Separate calculations were done with models in which the ionizable residues of the protein were in their neutral or ionized forms. Trajectories were propagated with time steps of 1 fs at 295 K, and the electrostatic energy difference between reactant and product electronic states, $\Delta V_{elec}(t)$, was evaluated every 10 steps.

The parameterization of the intramolecular force fields for BChl-*b* and BPh-*b* was refined by setting the optimal value of the bond length, bond angle, and torsional angle for each type of bond equal to the mean value for all of the bonds of that type in the four BChl-*b* and two BPh-*b* molecules in the *Rp. viridis* crystal structure. Forces for improper torsions were also used to restrain departures of the π systems from planarity.

The electrostatic energy change associated with moving an electron instantaneously from P to B at time t in a molecular dynamics trajectory includes the change in direct interactions of P and B with each other (ΔV_{QQ}) and with the atoms of the protein and crystallographic waters ($\Delta V_{Q\mu}$); it also includes the changes in interactions with induced dipoles in the protein and crystallographic waters (ΔV_{ind}), with induced dipoles on the grid of points representing the surroundings ($\Delta V_{H2O} + \Delta V_{memb}$), and with the bulk solvent surrounding the system (ΔV_{bulk}):

$$\Delta V_{elec}(t) = \Delta V_{QQ} + \Delta V_{Q\mu} + \Delta V_{ind} + \Delta V_{H_2O} + \Delta V_{memb} + \Delta V_{bulk} \quad (7)$$

In addition to the electrostatic energy, the total energy gap between the reactant and product, $\Delta V(t)$, includes the gas-phase energy change for electron transfer when the donor and acceptor are at infinite distance in a vacuum, ΔE_{gas}:

$$\Delta V(t) = \Delta V_{elec}(t) + \Delta E_{gas} \quad (8)$$

In evaluating $\bar{\mathcal{P}}(\Delta V)$, we can focus on $\Delta V_{elec}(t)$ because the constant term ΔE_{gas} does not affect the reorganization energy. To illustrate the calculated free energy surfaces for P*B and P^+B^-, we use an assumed ΔE_{gas} of 50.5 kcal/mol for the reaction $P^*B \rightarrow P^+B^-$, which makes the reaction weakly exothermic, in accord with the previous results cited above. The same value of ΔE_{gas} is used for all of the models considered, although estimates of this parameter depend somewhat on the details of the model (Alden et al., 1996a). Interactions between the two BChls of P are considered to be part of ΔE_{gas}, and therefore are not included in ΔV_{QQ} or ΔV_{ind}. These interactions are included, however, in the forces and energies for the molecular dynamics, as are the classical internal energies of the BChls. The histidine axial ligands of P and B are treated as part of the protein. Interactions with electrolytes in the medium are neglected.

To treat the effects of induced dipoles in the solvent, membrane, and outer regions of the protein (ΔV_{H_2O} and ΔV_{memb}), each point in the grid embedded in the microscopic system was assigned an induced dipole ($\vec{\mu}$) with a magnitude that depended on the field ($\vec{\xi}$) from the atomic charges and the other induced dipoles. To model a phospholipid membrane or an annulus of detergents, the grid elements in a 40-Å belt around the reaction center were assigned an electronic polarizability corresponding to a macroscopic dielectric constant of 2 (Alden et al., 1995). The grid elements in the polar regions on either side of the belt were assigned dielectric properties resembling those of bulk water. We also considered a model in which all of the grid points were treated as water dipoles. In previous Enzymix calculations, the dependence of $|\vec{\mu}|$ on $|\vec{\xi}|$ for water dipoles was described by a Langevin-type equation (Warshel and Russell, 1984; Russell and Warshel, 1985; Luzhkov and Warshel, 1992). Here we used an exponential

approximation of the Langevin equation: $|\vec{\mu}| = \alpha[1 - \exp(-\beta|\vec{\xi}|)]$, with $\alpha = 0.35\ e$Å and $\beta = 46.8\ e^{-1}$Å^2 (Alden et al., 1996b). A repulsive potential proportional to r^{-12} was used to prevent mobile atoms from impinging on the fixed grid points. To attenuate interactions with the nearest atoms, the field from dipole j on atom i was scaled by the factor $\{1 - \exp[-(r_{ij}/r_o)^4]\}$, where r_{ij} is the distance between the atom and grid point j and $r_o = 3$ Å. The same scaling was used to attenuate the interactions between neighboring induced dipoles.

The induced dipoles of the protein and the hydrophobic layer of the membrane were evaluated for the PB and P^+B^- electronic states once every 10 steps in the dynamics (on each calculation of ΔV_{elec}). These relatively weak, electronic dipoles were assumed to relax instantaneously in response to the fluctuating electric fields from the protein, electron carriers, and Langevin dipoles. An effective screening constant of 1.1 was used to correct approximately for interactions of the induced dipoles with each other (Russell and Warshel, 1985). The Langevin dipoles were evaluated once on each step in the dynamics, and their interactions with each other were treated explicitly. However, the Langevin dipoles were fixed during the evaluation of the energy change associated with moving an electron from P to B. This procedure models the comparatively slow dielectric relaxation of water or the polar head groups of membrane phospholipids. ΔV_{bulk} was evaluated with an expression given previously (Alden et al., 1996b), which again distinguishes between low- and high-frequency induced dipoles. Forces resulting from interactions with the bulk solvent were neglected for computation of accelerations during the molecular dynamics trajectories.

Before the trajectories described below, the system was equilibrated by molecular dynamics in the ground state (PB) for several picoseconds at 30 K and then for 20 ps at 295 K. An additional equilibration period of at least 2 ps in state P^+B^- was allowed before each of the trajectories in this state.

RESULTS AND DISCUSSION

Fig. 1 shows plots of the time-dependent electrostatic energy difference between the states PB and P^+B^-, $\Delta V_{elec}(t)$, during molecular dynamics trajectories in the two states. The model of the reaction center includes a membrane with polar and nonpolar regions, and all ionizable groups are taken to be neutral. Note that the mean value of ΔV_{elec} is more negative in P^+B^- than in PB; the difference reflects reorganization of the system in response to charge separation.

Table 1 lists the terms that contribute to ΔV_{elec}, as averaged over molecular dynamics trajectories on the PB and P^+B^- surfaces. Relaxations of the protein around the charged electron carriers make $\langle \Delta V_{Q\mu} \rangle$ more favorable in P^+B^- than in the ground state. Small movements of P and B with respect to each other also make $\langle \Delta V_{QQ} \rangle$ slightly more favorable in P^+B^-. However, the more negative values of $\langle \Delta V_{Q\mu} \rangle$ and $\langle \Delta V_{QQ} \rangle$ are offset by less negative values of $\langle \Delta V_{ind} \rangle$ and $\langle \Delta V_{H_2O} + \Delta V_{memb} \rangle$.

As discussed in the Methods section, the free energy functions Δg_1 and Δg_2 can be obtained as functions of the energy gap by first constructing histograms of the relative probability, $\bar{\mathcal{P}}(\Delta V)$, of finding various values of $\Delta V(t)$ during the two trajectories (Fig. 2). The free energy of the system in state s (P*B or P^+B^-) is given by

$$\Delta g(\Delta V) = -RT \ln\{\bar{\mathcal{P}}_s(\Delta V)\} + \Delta G_s^\circ \qquad (9)$$

where ΔG_s° is the standard free energy difference between state s and a reference state. We take the reference state to be P*B, so that $\Delta G_{P*B}^\circ = 0$, and simplify $\Delta G_{P^+B^-}^\circ$ to ΔG°. Given the probability functions for the two states, ΔG° is determined simply by setting $\Delta g_{P^+B^-}$ equal to Δg_{P*B} at $\Delta V = 0$.

The free energy functions obtained from the trajectories of Fig. 1 are shown in the top part of Fig. 3. In Marcus' (1956, 1996) treatment, the functions for the reactant and product state are assumed to have the same curvature. Because the actual $\Delta g_{P^+B^-}$ and Δg_{P*B} functions have somewhat different curvatures, there are several possible ways to

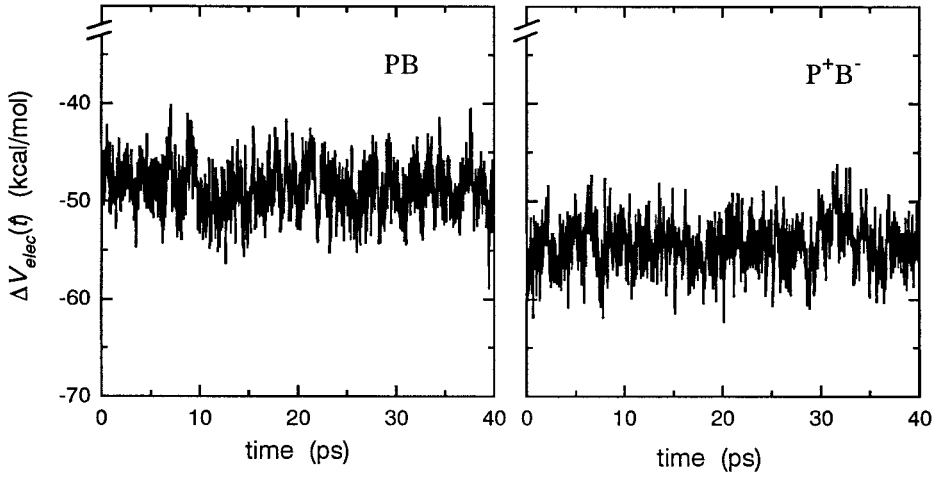

FIGURE 1 The time-dependent electrostatic energy gap between PB and P^+B^- during 40-ps trajectories at 295 K on the PB (*left*) and P^+B^- (*right*) potential surfaces. Each trajectory was preceded by an equilibration period in the same state. Ionizable amino acid side chains were treated as neutral. The potential energy surface of the ground-state PB is used as an approximation of the surface of the excited-state P*B (see text).

TABLE 1 Contributions to $\langle \Delta V_{elec} \rangle$ for P*B $\rightarrow$ P^+B^-*

s#	Model§	$\langle \Delta V_{QQ} \rangle_s$	$\langle \Delta V_{Q\mu} \rangle_s$	$\langle \Delta V_{ind} \rangle_s$	$\langle \Delta V_{H_2O/memb} \rangle_s$¶	$\langle \Delta V_{bulk} \rangle_s$	$\langle \Delta V_{elec} \rangle_s$
PB	n,m	−30.2	−7.7	−12.6	2.2	−0.2	−48.6
P^+B^-	n,m	−30.8	−13.5	−10.2	0.1	−0.0	−54.4
PB	i,m	−30.1	−11.8	−10.7	0.5	0.5	−51.6
P^+B^-	i,m	−30.5	−19.0	−8.0	0.0	0.4	−57.0
PB	n,w	−30.5	−6.9	−12.9	4.9	−0.4	−45.8
P^+B^-	n,w	−30.8	−14.8	−10.3	−1.5	−0.5	−57.8
PB	i,w	−30.1	−11.9	−10.7	3.8	−0.0	−48.9
P^+B^-	i,w	−30.2	−18.7	−8.4	−3.9	−0.1	−61.1

*Energies are given in kcal/mol.
#Electronic state in which the molecular dynamics trajectory was propagated. $\langle \ldots \rangle_s$ means an average over a trajectory in state s. The potential energy surface of the ground state PB is used as an approximation of the surface of the excited state P*B (see text).
§Ionizable amino acid side chains were either neutral (n) or ionized (i), and the reaction center was embedded in either a membrane (m) or water (w). The trajectory lengths for P^+B^- in the (i,m) and (i,w) models were 25 and 20 ps, respectively; all of the others were between 40 and 45 ps.
¶$\langle \Delta V_{H_2O} + \Delta V_{memb} \rangle$.

define the reorganization energy of the reaction. One possibility is to take the mean of the change in Δg_{P^*B} for moving P*B from $\Delta V^\circ_{P^*B}$ to $\Delta V^\circ_{P^+B^-}$ and the corresponding change for moving P^+B^- from $\Delta V^\circ_{P^+B^-}$ to $\Delta V^\circ_{P^*B}$. These quantities are indicated by the vertical arrows labeled λ_1 and λ_2 in Fig. 3. This definition gives $\lambda \approx 1.5$ kcal/mol (0.065 eV), with $\lambda_1 \approx 1.45$ and $\lambda_2 \approx 1.55$ kcal/mol. Because $\Delta g^\ddagger = (\Delta G^\circ + \lambda)^2/4\lambda$ in the Marcus theory, another possibility is to define λ as $4\Delta g^\ddagger_{(\Delta G^\circ = 0)}$, where $\Delta g^\ddagger_{(\Delta G^\circ = 0)}$ is the activation energy for the reaction when $\Delta G^\circ = 0$. The intersection of Δg_{P^*B} with $\Delta g_{P^+B^-} - \Delta G^\circ$ (not shown) gives $\Delta g^\ddagger_{(\Delta G^\circ = 0)} \approx 0.43$ kcal/mol and $\lambda \approx 1.7$ kcal/mol.

In the model used for the calculations described so far, all of the ionizable side chains were in their neutral states. The lower panel of Fig. 3 shows the results obtained when all of the ionizable chains were ionized. Although the mean values of ΔV_{elec} are more negative by 2–3 kcal/mol, the calculated reorganization energies are essentially the same as in the neutral model. With the value of ΔE_{gas} used here, $\Delta G^\circ \approx -0.6$ kcal/mol for P*B $\rightarrow$ P^+B^- in the neutral model, and −2.5 kcal/mol in the ionized model. In both models, the two curves intersect near the minimum for P*B, giving an activation energy of < 0.2 kcal/mol.

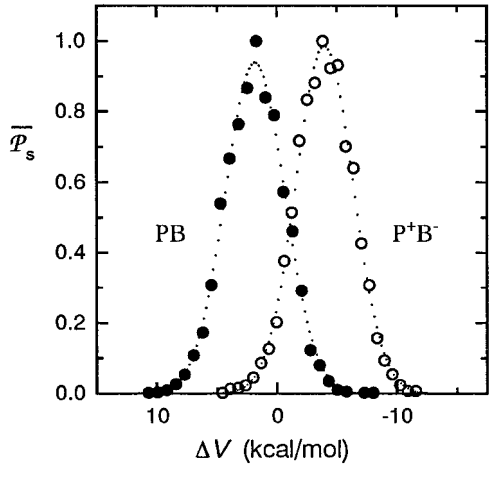

FIGURE 2 Distributions of the calculated energy gap between P*B and P^+B^- during the PB (●) and P^+B^- (○) trajectories shown in Fig. 1. The total energy gap (ΔV) includes, in addition to ΔV_{elec}, ΔE_{gas} for the reaction P*B $\rightarrow$ P^+B^- (50.5 kcal/mol). $\bar{\mathcal{P}}_s(\Delta V')$ is the relative probability that ΔV is within a small interval ($\pm\delta$) around the value $\Delta V'$, averaged over a trajectory in electronic state *s*. The bin size 2δ was chosen to divide the total range of ΔV for each trajectory into 25 equal intervals. The dotted curves are Gaussian fits.

Although the molecular dynamics trajectory for the reactant state P*B was actually propagated on the potential energy surface of the ground state (PB), relatively little reorganization of the system is expected to accompany excitation of P. The charge transfer character of P* is probably less than 10% (Parson and Warshel, 1987), and the dipole moments of intradimer charge transfer states are much smaller than the dipole moment of P^+B^-. In addition, the system has only a few picoseconds to reorganize in response to any change in dipole moment that does result from excitation.

A much larger reorganization energy is obtained if the entire medium surrounding the protein is modeled by Langevin-induced dipoles with the dielectric properties of bulk water. The Δg functions in this model seem notably anharmonic, and the function for P^+B^- has markedly greater curvature than that for P*B, so that the estimated values of λ_1 and λ_2 differ by ~4 kcal/mol (Fig. 4). The mean of λ_1 and λ_2 is on the order of 6.5 kcal/mol. As shown in Table 1, $\langle \Delta V_{H_2O} + \Delta V_{memb} \rangle$ in the water model is positive (unfavorable for charge separation) for P*B, but becomes negative for P^+B^-. Water dipoles that are oriented more or less randomly in state P*B evidently become much more tightly aligned in response to the field from P^+B^-. This model is probably less realistic, because relatively little bulk water will reside in the nonpolar belt of lipid surrounding the reaction center (Yeates et al., 1987; Roth et al., 1989), although the exact amount of water sequestered in small pockets of the protein merits futher investigation (Alden et al., 1995). As in the membrane model, trajectories with all

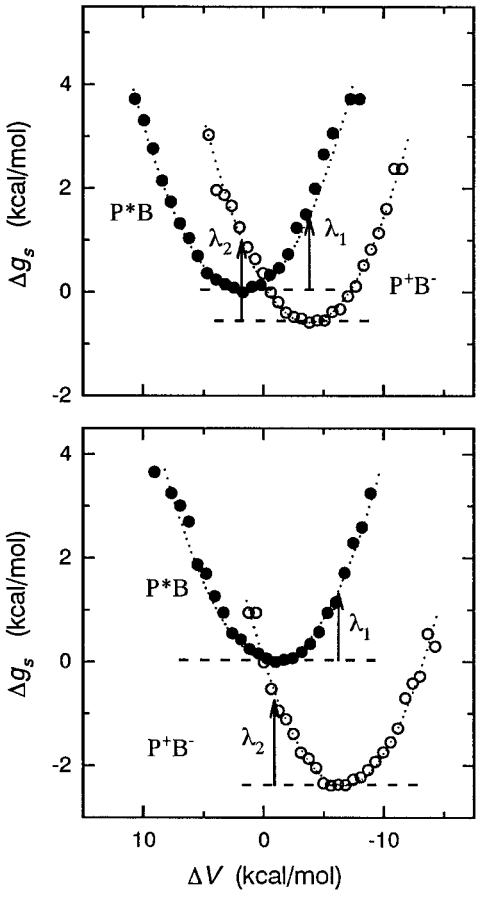

FIGURE 3 Calculated free energy functions of the reaction coordinate ΔV in states P*B (●) and P^+B^- (○). The free energies are referred to the minimum in state P*B. The vertical lines (λ_1 and λ_2) indicate the reorganization energies of the reactants and products. The upper panel is for a model in which the ionizable amino acid side chains are neutral; the lower panel is for a model with the ionizable groups charged. The dotted curves are parabolic fits. The Δg curve for P^+B^- in the lower panel is based on a trajectory of 25 ps after an equilibration period; all of the other curves represent 40-ps trajectories.

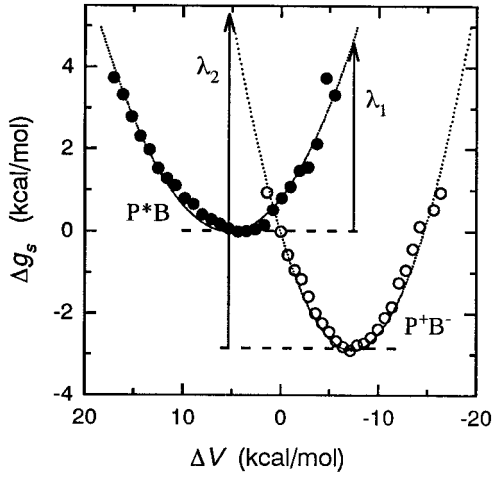

FIGURE 4 Free energy functions of ΔV in states P*B (●) and P^+B^- (○), calculated for a model in which the membrane surrounding the reaction center was replaced by water. The ionizable side chains were neutral. The trajectory lengths were 45 ps. ΔE_{gas} was taken to be 50.5 kcal/mol, as in Fig. 3. The dotted curves are parabolic fits.

of the ionizable groups charged gave essentially the same apparent reorganization energies (not shown).

If the time-dependent energy gap $\Delta V(t)$ is a Gaussian variable with standard deviation σ_s, the free energy function should be given by

$$\Delta g_s = \frac{\kappa_s}{2}(\Delta V - \Delta V_s^o)^2 + \Delta G_s^o \qquad (10)$$

with $\kappa_s = RT/\sigma_s$. The calculated functions are in good accord with this relationship. However, the free energy functions do not conform to Eq. 6, which should apply if the trajectories explored the entire configurational space of the system (see Methods). Fig. 5 illustrates the discrepancy for the model that includes a membrane and has all of the ionizable groups in their neutral forms; the results are similar in the other models. The free energy function calculated with Eq. 6 (*curve 2′*) gives larger values of $\Delta G°$ and λ than the function obtained directly from a trajectory in state P^+B^- (*curve 2*). Note that the disagreement with Eq. 6 does not hinge on the choice of ΔE_{gas}, which affects only the vertical positioning of P^+B^-; it lies in the horizontal separation of the two minima ($\Delta V^\circ_{P*B} - \Delta V^\circ_{P^+B^-}$). If both Δg curves are described by Eq. 10 with the same curvature (κ), Eq. 6 would require that $\Delta V^\circ_{P*B} - \Delta V^\circ_{P^+B^-} = 1/\kappa$. For the membrane model with the ionizable groups neutral, we found $\kappa_{P*B} = 0.095$ and $\kappa_{P^+B^-} = 0.103$ mol/kcal, giving $1/\kappa \approx 10$ kcal/mol. The actual separation is only ~5.5 kcal/mol.

The discrepancy between the observed values of $\Delta V^\circ_{P*B} - \Delta V^\circ_{P^+B^-}$ and the values predicted by Eq. 6 probably reflects the fact that finite trajectories on the P*B and P^+B^- potential energy surfaces necessarily explore limited and, to

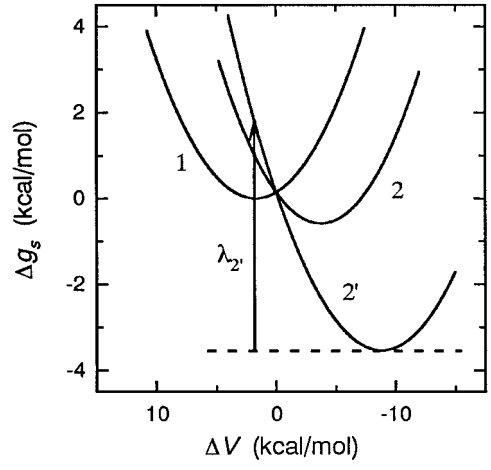

FIGURE 5 Parabolic fits to the free energy functions $\Delta g_{P^+B^-}$ (*curve 1*) and Δg_{P*B} (*curve 2*) in the upper panel of Fig. 3, and (*curve 2′*) the free energy function for P^+B^-, calculated by Eq. 6 from the parabolic function for P*B. The reorganization energy calculated from curves 1 and 2′ ($\lambda_{2'}$) is 5.3 kcal/mol. The smaller value of ~1.5 kcal/mol obtained from curves 1 and 2 is probably a better estimate of the effective λ.

some extent, nonoverlapping regions of configurational space. There are two points to consider here. First, reaction centers in the state P*B are unlikely to visit all of the conformations that are adopted by reaction centers in P^+B^-, and vice versa. The simulation time needed for proper sampling of the relevant conformational regions of P^+B^- during a trajectory on P*B will, therefore, be longer than the time required during a trajectory on P^+B^- itself. Second, even a trajectory on P^+B^- will not sample all of the conformations that are ultimately significantly populated in this state, if the simulation time is shorter than the time required for the system to approach conformational equilibrium after charge separation.

The conformational equilibration time is not necessarily related in any simple way to the time needed to sample the pertinent conformational space of P^+B^- during a trajectory in P*B, although barriers to conformational fluctuations would impede both equilibration and sampling. Experimental measurements of vibrational coherences after excitation of reaction centers with femtosecond flashes have shown that complete conformational equilibration is not achieved on the 3-ps time scale of the initial charge separation (Vos et al., 1994a,b; Woodbury et al., 1994; Stanley and Boxer, 1995). Many conformational changes in proteins occur on nanosecond or even longer time scales. This implies that the effective values of λ and ΔG° for the charge separation reactions are functions of time and, presumably, of temperature. Although FEP techniques can be used to enforce equilibrium in a computer model (Hwang and Warshel, 1987; Kuharski et al., 1988; King and Warshel, 1990; Warshel and Parson, 1991; Kollman, 1993), the estimates of $\lambda \approx 1.5$ kcal/mol obtained from the free energy functions shown in Fig. 3 or 1.7 kcal/mol obtained from $\Delta g^{\ddagger}_{(\Delta G^\circ = 0)}$ probably are more pertinent to the initial electron transfer kinetics than values obtained for a fully equilibrated system. Conformational relaxations that occur on time scales of more than 10 ps will have little bearing on the kinetics. As long as the electronic coupling between P*B and P^+B^- is sufficiently weak so that reversibility can be neglected (i.e., as long as the reaction is nonadiabatic), the kinetics can probably be simulated best by using the semiclassical trajectory method to evaluate the rate of surface hopping (Creighton et al., 1988; Warshel and Parson, 1991; Parson and Warshel, 1995). The situation may be different, however, in the second step of charge separation, where the coupling between P^+B^-H and P^+BH^- may be stronger. Here conformational relaxations of P^+H^- could be important for pulling the reaction to completion (Kitzing and Kuhn, 1990; Peloquin et al., 1994; Woodbury et al., 1994).

In addition to giving larger reorganization energies, FEP calculations should give more negative values of ΔG° compared to calculations that do not enforce conformational equilibrium. Because the activation energy depends on $\Delta G^\circ + \lambda$, the rate constants obtained by using the Marcus relationship with the two sets of values for ΔG° and λ may be similar. The same is true for calculations in which Δg_2 is obtained either directly or from Δg_1 by Eq. 6. The identical activation energies associated with curves 2 and 2′ in Fig. 5 illustrate this point.

In conclusion, molecular dynamics simulations using the *Rp. viridis* crystal structure and using a model in which the reaction center is embedded in a membrane give a reorganization energy of 1.6 ± 0.2 kcal/mol for the initial step of charge separation. The calculated reorganization energy is insensitive to the treatment of the ionizable side chains. Taken with recent evidence that P^+B^- lies slightly below P* in energy, the small size of λ is in good accord with the high speed of the reaction and with the observation that the rate is insensitive to temperature. The small reorganization energy depends on the low polarizability of the membrane: similar calculations using a model in which the reaction center is surrounded by water give a reorganization energy on the order of 6.5 kcal/mol. Calculations based on Eq. 6 probably lead to an overestimate of λ, because a trajectory in the reactant state does not sample all of the conformational states that become important in the products. And finally, because the system evidently does not relax completely on the time scale of the initial electron transfer steps, both λ and ΔG° should be considered functions of time and temperature.

We thank the National Science Foundation (grant MCB-9111599) and the National Institutes of Health (grant GM-40283) for support, and R. Alden and V. Nagarajan for helpful discussion.

REFERENCES

Alden, R. G., W. W. Parson, Z. T. Chu, and A. Warshel. 1995. Calculations of electrostatic energies in photosynthetic reaction centers. *J. Am. Chem. Soc.* 117:12284–12298.

Alden, R. G., W. W. Parson, Z. T. Chu, and A. Warshel. 1996a. Macroscopic and microscopic estimates of the energetics of charge separation in bacterial reaction centers. *In* Reaction Centers of Photosynthetic Bacteria: Structure and Dynamics. M. E. Michel-Byerle, editor. Springer-Verlag, Berlin. 105–116.

Alden, R. G., W. W. Parson, Z. T. Chu, and A. Warshel. 1996b. Orientation of the OH dipole of tyrosine (M)210 and its effect on electrostatic energies in photosynthetic bacterial reaction centers. *J. Phys. Chem.* 100:16761–16770.

Arlt, T., B. Dohse, S. Schmidt, J. Wachtveitl, E. Laussermaier, W. Zinth, and D. Oesterhelt. 1996. Electron transfer dynamics of *Rhodopseudomonas viridis* reaction centers with a modified binding site for the accessory bacteriochlorophyll. *Biochemistry.* 35:9235–9244.

Arlt, T., S. Schmidt, W. Kaiser, C. Lauterwasser, M. Meyer, H. Scheer, and W. Zinth. 1993. The accessory bacteriochlorophyll: a real electron carrier in primary photosynthesis. *Proc. Natl. Acad. Sci. USA.* 90: 11757–11762.

Bixon, M., J. Jortner, and M. E. Michel-Beyerle. 1996. Energetics of the primary charge separation in bacterial photosynthesis. *In* Reaction Centers of Photosynthetic Bacteria: Structure and Dynamics. M. E. Michel-Byerle, editor. Springer-Verlag, Berlin. 287–296.

Breton, J., J.-L. Martin, G. R. Fleming, and J.-C. Lambry. 1988. Low temperature femtosecond spectroscopy of the initial step of electron transfer in reaction centers from photosynthetic purple bacteria. *Biochemistry.* 27:8276–8284.

Creighton, S., J.-K. Hwang, A. Warshel, W. W. Parson, and J. Norris. 1988. Simulating the dynamics of the primary charge separation process in bacterial photosynthesis. *Biochemistry.* 27:774–781.

Deisenhofer, J., O. Epp, I. Sinning, and H. Michel. 1995. Crystallographic refinement at 2.3 Å resolution and refined model of the photosynthetic

reaction center from *Rhodopseudomonas viridis*. *J. Mol. Biol.* 246: 429–457.

Egger, R., and C. H. Mak. 1993. Dynamical effects in the calculation of quantum rates for electron transfer reactions. *J. Chem. Phys.* 99: 2541–2549.

Egger, R., and C. H. Mak. 1994. Dissipative three-state system and the primary electron transfer in the bacterial photosynthetic reaction center. *J. Phys. Chem.* 98:9903–9918.

Fleming, G. R., J.-L. Martin, and J. Breton. 1988. Rates of primary electron transfer in photosynthetic reaction centers and their mechanistic implications. *Nature.* 33:190–192.

Goldstein, R. A., L. Takiff, and S. G. Boxer. 1988. Energetics of initial charge separation in bacterial photosynthesis: the triplet decay rate in very high magnetic fields. *Biochim. Biophys. Acta.* 934:253–263.

Gunner, M., A. Nichols, and B. Honig. 1996. Electrostatic potentials in *Rhodopseudomonas viridis* reaction centers: implications for the driving force and directionality of electron transfer. *J. Phys. Chem.* 100: 4277–4291.

Hamm, P., K. A. Gray, D. Oesterhelt, R. Feick, H. Scheer, and W. Zinth. 1993. Subpicosecond emission studies of bacterial reaction centers. *Biochim. Biophys. Acta.* 1142:99–105.

Heller, B. A., D. Holten, and C. Kirmaier. 1995. Control of electron transfer between the L- and M-sides of the photosynthetic reaction center. *Science.* 269:940–945.

Heller, B. A., D. Holten, and C. Kirmaier. 1996. Effects of Asp residues near the L-side pigments in bacterial reaction centers. *Biochemistry.* 35:15418–15427.

Holzapfel, W., U. Finkele, W. Kaiser, D. Oesterhelt, H. Scheer, H. U. Stilz, and W. Zinth. 1990. Initial electron transfer in the reaction center from *Rhodobacter sphaeroides*. *Proc. Natl. Acad. Sci. USA.* 87:5168–5172.

Holzwarth, A. R., and M. G. Muller. 1996. Energetics and kinetics of radical pairs in reaction centers from *Rhodobacter sphaeroides.* A femtosecond transient absorption study. *Biochemistry.* 35:11820–11831.

Huber, M., M. Meyer, T. Nägele, I. Hartl, H. Scheer, W. Zinth, and J. Wachtveitl. 1995. Primary photosynthesis in reaction centers containing four different types of electron acceptors at site H_A. *Chem. Phys. Lett.* 197:297–305.

Hwang, J.-K., and A. Warshel. 1987. Microscopic examination of free energy relationships for electron transfer in polar solvents. *J. Am. Chem. Soc.* 109:715–720.

Hwang, J.-K., and A. Warshel. 1997. On the relationship between the dispersed polaron and spin-boson models. *Chem. Phys. Lett.* 271: 223–225.

Jia, Y., T. J. DiMagno, C.-K. Chan, Z. Wang, M. Du, D. K. Hanson, M. Schiffer, J. R. Norris, G. R. Fleming, and M. S. Popov. 1993. Primary charge separation in mutant reaction centers of *Rhodobacter capsulatus. J. Phys. Chem.* 97:13180–13191.

Kennis, J. T. M., A. Y. Shkuropatov, I. H. M. van Stokkum, P. Gast, A. J. Hoff, V. A. Shuvalov, and T. J. Aartsma. 1997. *Biochemistry.* (in press).

King, G., F. S. Lee, and A. Warshel. 1991. Microscopic simulations of macroscopic dielectric constants of solvated proteins. *J. Chem. Phys.* 95:4366–4377.

King, G., and A. Warshel. 1990. Investigation of the free energy function for electron transfer reactions. *J. Chem. Phys.* 93:8682–8692.

Kirmaier, C., L. Laporte, C. C. Schenck, and D. Holten. 1995a. The nature and dynamics of the charge-separated intermediate in reaction centers in which bacteriochlorophyll replaces the photoactive bacteriopheophytin. 1. Spectral characterization of the transient state. *J. Phys. Chem.* 99: 8903–8909.

Kirmaier, C., L. Laporte, C. C. Schenck, and D. Holten. 1995b. The nature and dynamics of the charge-separated intermediate in reaction centers in which bacteriochlorophyll replaces the photoactive bacteriopheophytin. 2. The rates and yields of charge separation and recombination. *J. Phys. Chem.* 99:8910–8917.

Kitzing, E. V., and H. Kuhn. 1990. Primary electron transfer in photosynthetic reaction centers. *J. Phys. Chem.* 94:1699–1702.

Kollman, P. A. 1993. Free energy calculations: applications to chemical and biochemical phenomena. *Chem. Rev.* 93:2395–2417.

Kuharski, R. A., J. S. Bader, D. Chandler, M. Sprik, M. Klein, and R. Impey. 1988. Molecular model for aqueous ferrous-ferric electron transfer. *J. Chem. Phys.* 89:3248–3256.

Lee, F. S., Z. T. Chu, and A. Warshel. 1993. Microscopic and semimicroscopic calculations of electrostatic energies in proteins by the POLARIS and ENZYMIX programs. *J. Comp. Chem.* 14:161–185.

Lee, F. S., and A. Warshel. 1992. A local reaction field method for fast evaluation of long-range electrostatic interactions in molecular simulations. *J. Chem. Phys.* 97:3100–3107.

Luzhkov, V., and A. Warshel. 1992. Microscopic models for quantum mechanical calculations of chemical processes in solutions: LD/AMPAC and SCAAS/AMPAC calculations of solvation energies. *J. Comp. Chem.* 13:199–213.

Maiti, S., G. C. Walker, B. R. Cowen, R. Pippenger, C. C. Moser, P. L. Dutton, and R. M. Hochstrasser. 1994. Femtosecond coherent transient infrared spectroscopy of reaction centers from *Rhodobacter sphaeroides. Proc. Natl. Acad. Sci. USA.* 91:10360–10364.

Makri, N., E. J. Sim, D. E. Makarov, and M. Topaler. 1996. Long-time quantum simulation of the primary charge separation in bacterial photosynthesis. *Proc. Natl. Acad. Sci. USA.* 93:3926–3931.

Marchi, M., J. N. Gehlen, D. Chandler, and M. Newton. 1993. Diabatic surfaces and the pathway for primary electron transfer in a photosynthetic reaction center. *J. Am. Chem. Soc.* 115:4178–4190.

Marcus, R. 1956. On the theory of oxidation-reduction reactions involving electron transfer. *J. Phys. Chem.* 24:966–978.

Marcus, R. 1996. Electron transfer reactions in chemistry. Theory and experiment. *In* Protein Electron Transfer. D. S. Bendall, editor. Bios Scientific Publishers, Oxford. 249–272.

Miller, W. H., and T. F. George. 1972. Semiclassical theory of electronic transitions in low energy atomic and molecular collisions involving several nuclear degrees of freedom. *J. Chem. Phys.* 56:5637–5652.

Muegge, I., P. X. Qi, A. J. Wand, Z. T. Chu, and A. Warshel. 1997. The reorganization energy of cytochrome c revisited. *J. Phys. Chem.* 101: 825–836.

Murchison, H. A., R. G. Alden, J. P. Allen, J. M. Peloquin, A. K. W. Taguchi, N. W. Woodbury, and J. C. Williams. 1993. Mutations designed to modify the environment of the primary electron donor of the reaction center from *Rhodobacter sphaeroides*: phenylalanine to leucine at L167 and histidine to phenylalanine at L186. *Biochemistry.* 32: 3498–3505.

Nagarajan, V., W. W. Parson, D. Davis, and C. C. Schenck. 1993. Kinetics and free energy gaps of electron transfer reactions in *Rhodobacter sphaeroides* reaction centers. *Biochemistry.* 32:12324–12336.

Ogrodnik, A., W. Keupp, M. Volk, G. Auermeier, and M. E. Michel-Beyerle. 1994. Inhomogeneity of radical pair energies in photosynthetic reaction centers revealed by differences in recombination dynamics of $P^+H_A^-$ when detected in delayed emission and in absorption. *J. Phys. Chem.* 98:3432–3439.

Ogrodnik, A., M. Volk, R. Letterer, R. Feik, and M. E. Michel-Beyerle. 1988. Determination of free energies in reaction centers of *Rb. sphaeroides. Biochim. Biophys. Acta.* 936:361–371.

Parson, W. W., Z. T. Chu, and A. Warshel. 1990. Electrostatic control of charge separation in bacterial photosynthesis. *Biochim. Biophys. Acta.* 1017:251–272.

Parson, W. W., V. Nagarajan, D. Gaul, C. C. Schenck, Z. T. Chu, and A. Warshel. 1990. Electrostatic effects on the speed and directionality of electron transfer in bacterial reaction centers: the special role of tyrosine M-208. *In* Reaction Centers of Photosynthetic Bacteria. M. E. Michel-Byerle, editor. Springer-Verlag, Berlin. 239–249.

Parson, W. W., and A. Warshel. 1987. Spectroscopic properties of photosynthetic reaction centers. 2. Application of the theory to *Rhodopseudomonas viridis*. *J. Am. Chem. Soc.* 109:6152–6163.

Parson, W. W., and A. Warshel. 1995. Theoretical analyses of electron-transfer reactions. *In* Anoxygenic Photosynthetic Bacteria. R. E. Blankenship, M. T. Madigan, and C. E. Bauer, editors. Kluwer Academic Publishers, Dordrecht, the Netherlands. 559–575.

Peloquin, J. M., J. C. Williams, X. Lin, R. G. Alden, A. K. W. Taguchi, J. P. Allen, and N. W. Woodbury. 1994. Time-dependent thermodynamics during early electron transfer in reaction centers from *Rhodobacter sphaeroides*. *Biochemistry.* 33:8089–8100.

Roth, M., A. Lewit-Bentley, H. Michel, J. Deisenhofer, and R. Huber. 1989. Detergent structure in crystals of a bacterial photosynthetic reaction center. *Nature.* 340:659–662.

Russell, S. T., and A. Warshel. 1985. Calculations of electrostatic energies in proteins. The energetics of ionized groups in BPTI. *J. Mol. Biol.* 185:389–404.

Schmidt, S., T. Arlt, P. Hamm, H. Huber, T. Nägele, J. Wachtveitl, M. Meyer, H. Scheer, and W. Zinth. 1994. Energetics of the primary electron transfer reaction revealed by ultrafast spectroscopy on modified bacterial reaction centers. *Chem. Phys. Lett.* 223:116–120.

Schmidt, S., T. Arlt, P. Hamm, H. Huber, T. Nägele, J. Wachtveitl, M. Meyer, H. Scheer, and W. Zinth. 1995. Primary electron-transfer dynamics in modified bacterial reaction centers containing pheophytin-a instead of bacteriopheophytin-a. *Spectrochim. Acta.* 51A:1565–1578.

Schulten, K., and M. Tesch. 1991. Coupling of protein motion to electron transfer: molecular dynamics and stochastic quantum mechanics study of photosynthetic reaction centers. *Chem. Phys.* 158:421–446.

Shkuropatov, A. Ya., and V. A. Shuvalov. 1996. Femtosecond kinetics of electron transfer in the bacteriochlorophyll (M)-modified reaction centers from *Rhodobacter sphaeroides* (R-26). *FEBS Lett.* 322:168–172.

Stanley, R. J., and S. G. Boxer. 1995. Oscillations in spontaneous fluorescence from photosynthetic reaction centers. *J. Phys. Chem.* 99:859–863.

Tachiya, M. 1989. Relation between the electron transfer rate and the free energy change of reaction. *J. Phys. Chem.* 93:7050–7052.

Tully, J. C., and R. M. Preston. 1971. Trajectory surface hopping approach to nonadiabatic molecular collisions: the reaction of H^+ with D_2. *J. Chem. Phys.* 55:562–572.

Van Brederode, M. E., L. M. P. Beekman, D. Kuciauskas, M. R. Jones, I. H. M. van Stokkum, and R. van Grondelle. 1996. Characteristics of the electron transfer reactions in the M210W reaction centre only mutant of *Rhodobacter sphaeroides*. *In* The Reaction Centers of Photosynthetic Bacteria: Structure and Dynamics. M. E. Michel-Byerle, editor. Springer-Verlag, Berlin. 225–237.

Vos, M. H., M. R. Jones, C. N. Hunter, J. Breton, J.-C. Lambry, and J.-L. Martin. 1994a. Coherent dynamics during the primary electron-transfer reaction in membrane-bound reaction centers of *Rhodobacter sphaeroides. Biochemistry.* 33:6750–6757.

Vos, M. H., M. R. Jones, C. N. Hunter, J. Breton, J.-L. Martin. 1994b. Coherent nuclear dynamics at room temperature in bacterial reaction centers. *Proc. Natl. Acad. Sci. USA.* 91:12701–12705.

Warshel, A. 1982. Dynamics of reactions in polar solvents. Semiclassical trajectory studies of electron transfer and proton transfer reactions. *J. Phys. Chem.* 86:2218–2224.

Warshel, A., Z. T. Chu, and W. W. Parson. 1989. Dispersed polaron simulations of electron transfer in photosynthetic reaction centers. *Science.* 246:112–116.

Warshel, A., Z. T. Chu, and W. W. Parson. 1994. On the energetics of the primary electron-transfer process in bacterial reaction centers. *Photochem. Photobiol. A. Chem.* 82:123–128.

Warshel, A., and J.-K. Hwang. 1985. Quantized semiclassical trajectory approach for evaluation of vibronic transitions in harmonic molecules. *J. Chem. Phys.* 82:1756–1771.

Warshel, A., and J.-K. Hwang. 1986. Simulation of the dynamics of electron transfer reactions in polar solvents: semiclassical trajectories and dispersed polaron approaches. *J. Chem. Phys.* 84:4938–4957.

Warshel, A., and W. W. Parson. 1991. Computer simulations of electron-transfer reactions in solution and in photosynthetic reaction centers. *Annu. Rev. Phys. Chem.* 42:279–309.

Warshel, A., and S. T. Russell. 1984. Calculations of electrostatic interactions in biological systems and solutions. *Q. Rev. Biophys.* 17:283–422.

Warshel, A., F. Sussman, and G. King. 1986. The free energies of charges in solvated proteins. Microscopic calculations using a reversible charging process. *Biochemistry.* 25:8368–8372.

Webster, F., E. T. Wang, P. J. Rossky, and R. A. Friesner. 1994. Stationary phase surface hopping for nonadiabatic dynamics. *J. Chem. Phys.* 100: 4835–4847.

Williams, J. C., R. G. Alden, H. A. Murchison, J. M. Peloquin, N. W. Woodbury, and J. P. Allen. 1992. Effects of mutations near the bacteriochlorophylls in reaction centers from *Rhodobacter sphaeroides*. *Biochemistry.* 31:11029–11037.

Woodbury, N. W. T., M. Becker, D. Middendorf, and W. W. Parson. 1985. Picosecond kinetics of the initial photochemical electron transfer reaction in bacterial photosynthetic reaction centers. *Biochemistry.* 24: 7516–7521.

Woodbury, N. W. T., and W. W. Parson. 1984. Nanosecond fluorescence from isolated photosynthetic reaction centers of *Rhodopseudomonas sphaeroides*. *Biochim. Biophys. Acta.* 767:345–361.

Woodbury, N. W., J. M. Peloquin, R. G. Alden, X. Lin, A. K. W. Taguchi, J. C. Williams, and J. P. Allen. 1994. Relationship between thermodynamics and mechanism during photoinduced charge separation in reaction centers from *Rhodobacter sphaeroides*. *Biochemistry.* 33: 8101–8112.

Yeates, T. O., H. Komiya, D. Rees, J. P. Allen, and G. Feher. 1987. Structure of the reaction center from *Rhodobacter sphaeroides* R-26: membrane-protein interactions. *Proc. Natl. Acad. Sci. USA.* 84: 6438–6442.

Zhou, H.-X., and A. Szabo. 1995. Microscopic formulation of Marcus' theory of electron transfer. *J. Chem. Phys.* 103:3481–3494.